SANDIA REPORT

SAND2015-
Unlimited Release
Printed May 2017

Turbulent Spot Pressure Fluctuation Wave Packet Model

Lawrence J. DeChant

Prepared by
Sandia National Laboratories
Albuquerque, New Mexico 87185 and Livermore, California 94550

Sandia National Laboratories is a multi-program laboratory managed and operated by Sandia Corporation, a wholly owned subsidiary of Lockheed Martin Corporation, for the U.S. Department of Energy's National Nuclear Security Administration under contract DE-AC04-94AL85000.

Issued by Sandia National Laboratories, operated for the United *S*tates Department of Energy by Sandia Corporation.

Available to DOE and DOE contractors from
U.S. Department of Energy
Office of Scientific and Technical Information
P.O. Box 62
Oak Ridge, TN 37831

Telephone: (865) 576-8401
Facsimile: (865) 576-5728
E-Mail: reports@adonis.osti.gov
Online ordering: http://www.osti.gov/bridge

Available to the public from
U.S. Department of Commerce
National Technical Information Service
5285 Port Royal Rd.
Springfield, VA 22161

Telephone: (800) 553-6847
Facsimile: (703) 605-6900
E-Mail: orders@ntis.fedworld.gov
Online order: http://www.ntis.gov/help/ordermethods.asp?loc=7-4-0#online

SAND2017-5749
Printed May 2017 2015

Turbulent Spot Pressure Fluctuation Wave Packet Model

Lawrence J. DeChant
Aerosciences Department
Sandia National Laboratories
P.O. Box 5800
Albuquerque, New Mexico 87185-0825

ABSTRACT

Wave packet analysis provides a connection between linear small disturbance theory and subsequent nonlinear turbulent spot flow behavior. The traditional association between linear stability analysis and nonlinear wave form is developed via the method of stationary phase whereby asymptotic (simplified) mean flow solutions are used to estimate dispersion behavior and stationary phase approximation are used to invert the associated Fourier transform. The resulting process typically requires nonlinear algebraic equations inversions that can be best performed numerically, which partially mitigates the value of the approximation as compared to a more complete, e.g. DNS or linear/nonlinear adjoint methods. To obtain a simpler, closed-form analytical result, the complete packet solution is modeled via approximate amplitude (linear convected kinematic wave initial value problem) and local sinusoidal (wave equation) expressions. Significantly, the initial value for the kinematic wave transport expression follows from a separable variable coefficient approximation to the linearized pressure fluctuation Poisson expression. The resulting amplitude solution, while approximate in nature, nonetheless, appears to mimic many of the global features, e.g. transitional flow intermittency and pressure fluctuation magnitude behavior. A low wave number wave packet models also recover meaningful auto-correlation and low frequency spectral behaviors.

ACKNOWLEDGMENTS

The authors would like to thank Justin Smith and Katya Casper; Aeroscience Department, Sandia National Laboratories for the research that provides the basis of this analysis. Technical insight and support from, R. Field, Component Science and Mechanics Department and Mikhail Mesh, Analytical Structural Dynamics Department; Sandia National Laboratories is greatly appreciated.

CONTENTS

FIGURES

NOMENCLATURE

Symbols

const	Constant
c	Velocity parameter definition (L/t)
c_0	Pressure model fluctuation constant
c_f	Skin friction coefficient
K	Wave number (1/L)
L	Streamwise length scale (L)
L_t	Transition zone streamwise length (L)
M	Mach number
p	Fluctuating pressure (m/Lt^2) or fluctuating pressure/density (L^2/t^2) (density modified)
p_0	Fluctuating pressure model initial condition (L^2/t^2) (density modified)
p_{trans}	Root mean square transition zone fluctuating pressure (L^2/t^2) (density modified)
p_{FD}	Root mean square fully-developed turbulent (post transition) fluctuating pressure (m/Lt^2)

	(density modified)
R	Dimensionless pressure correlation
t	Time (t)
u	Fluctuating streamwise velocity (L/t)
U	Mean streamwise velocity (L/t)
v	Fluctuating cross-stream velocity (L/t)
v^*	Friction velocity (L/t)
V_{rms}	Root mean square velocity fluctuation (L/t)
w	Lateral fluctuating velocity (L/t)
x	Streamwise spatial location (L)
x_i	Streamwise spot/packet location (L)
y	Cross-stream spatial location (L)

Greek

α_0	Local variable definition: $\alpha_0 = \frac{1}{c_0}\left(\frac{U}{v^*}\right)\left(\frac{\delta}{L_t}\right)$
β_0	Local variable definition $\beta_0 = k\delta\left(\frac{\delta}{L_t}\right)$
δ	Boundary layer thickness length scale (L)
η	Method-of-characteristics cross-stream location definition (L)
γ	Turbulent intermittency
κ	Dimensionless proportionality constant
λ	Separation constant ($1/L^2$)
μ	Separation constant ($1/L^2$)
φ	Spot shape angle
ω	Frequency (1/t)
ρ	Density (m/L^3)
Φ	Dimensionless pressure power spectral density: $\frac{U_\infty}{\delta^*}\Phi_{pp}\left(\frac{1}{2}\rho U_\infty^2\right)^{-2}$
τ	Temporal correlation function separation time scale (t)
τ_w	Wall shear stress
ξ	Method-of-characteristics streamwise location definition (L)

Subscripts/Superscripts

0	Constant value
∞	Free stream
inc	Incompressible
w	Wall value

I. INTRODUCTION

Wave packet analysis can be useful in providing a model for turbulent spot behavior in laminar turbulent transition. The connection between linear stability analysis and wave form via the method of stationary phase[1] is developed by Bowles and Smith[2] and Schmid and Henningson[3]. The method follows by combining a local (for example piecewise) mean flow solution with the method of stationary phase, whereby it is possible to estimate the shape and behavior of wave packets that are surrogates for turbulent spots. Corroboration of analytical models follows from the measurements and Cohen, Breuer and Haritonidis[4] which suggest good agreement between linear theory and measurement for packets prior to later time nonlinear interaction. Late time nonlinear behavior can also be examined using wave packet concepts as developed but experimentally and analytically by Kachanov and Lechenko[5] and more recently by Breuer, Cohen and Haritonidis[6]. Unfortunately, while traditional wave packet/method-of-stationary-phase model provides an elegant connection between linear stability theory and transitional flow behavior; this type of analysis yields complex results that (beyond rough estimates of spot shape) that may not be readily utilized in practical transitional flow analyses.

To provide a bridge between the more rigorous wave analyses and a simplified but explicit model we approximately solve the linearized Euler equations. We analyze these equations in context of a traditional wave packet approximation using a kinematic wave initial value problem formulation. The initial value for this computation follows from a modified pressure Poisson equation formulation. Indeed, while the connection between velocity fluctuation and pressure fluctuation is, of course, formally described by the pressure-Poisson equation we utilize a simple semi-empirical linearized expression[7,8] to map between pressure fluctuation and velocity fluctuation. Streamwise variation of the meanflow component is also explicitly included. Solving the resulting linear variable coefficient partial differential equation provides a plausible wave packet initial amplitude expression. Combination with the convective dominated kinematic wave solution results in an unsteady packet amplitude model. For a given wave number, the internal structure of the packet is shown to be consisting with a sinusoidal structure. This overall packet model is then extended to honor the streamwise growth of the disturbance.

Access to the wave packet pressure fluctuation model permits simplified, but physics-based modeling for the transition layer pressure field. Focusing on streamwise behavior only, a steady state amplitude distribution of pressure disturbances yields an overall pressure field that is broadly consistent with globally based root-mean-square fluctuation models[9] An estimate for the intermittency suggests good

agreement with traditional models[10,11,12] Finally focusing on small wavenumber/low frequency behavior, the wave packet model can be used to estimate a pressure fluctuation auto-correlation and frequency spectrum. Application of the model to these problems suggests that, even though the wave packet model derived here is certainly approximate in nature, it provides a simple explicit formulation for pressure behavior.

II. ANALYSIS

We start by developing the pressure fluctuation wave packet model by posing and solving the kinematic wave initial value problem. We then extend the model to include streamwise growth behavior.

A. Elementary Wave Packet Model

Consider the 3-d linearized Euler equations[2] for the fluctuating velocities u, v, w and the fluctuating pressure p.

$$\begin{aligned} &u_x + v_y + w_z = 0 \\ &u_t + Uu_x + vU_y + wU_z = -p_x \\ &v_t + Uv_x = -p_y \\ &w_t + Uw_x = -p_z \end{aligned} \tag{1}$$

The mean flow velocity is given as U. In our analysis we implicitly map the constant density into the pressure term. Notice as well, that we have included a small "z" component through the term: $U_z = \frac{\partial U}{\partial z}$.

These linear equations can be rewritten in terms of a single variable. Traditionally we focus on pressure p and v. Since the expressions are so well known[3] we'll simply quote the results. The pressure (fluctuation) is governed by (this expression follows from differentiating the 3 Euler equations by x, y, z and applying continuity):

$$p_{xx} + p_{yy} + p_{zz} = \nabla^2 p = -U_y v_x - U_z w_x \tag{2}$$

Equation (2) clearly requires a closure for the velocity derivative term: $v_x = \frac{\partial v}{\partial x}$ and $w_x = \frac{\partial w}{\partial x}$. The absence of explicit temporal terms in equation (2) suggests that an approximate solution may provide a useful estimate for initial condition behavior associated with a kinematic wave packet formulation.

For the purpose of estimating this wave packet initial condition magnitude description of the pressure in terms of the velocity fluctuation may make more sense. Following Lowson[7,8] the pressure fluctuation magnitude (for isotropic turbulence) has been given by:

$$p_{rms} = 0.58V_{rms}^2 \approx 0.7V_{rms}^2 \tag{3}$$

where p_{rms} is the root mean square magnitude of the pressure fluctuation. The density term here is again suppressed. Other models[8] utilize the friction velocity v^*. Note that for isotropic turbulence $V_{rms} = u = v = w$. Thus we could write:

$$p = c_0 v_0^* v \rightarrow v_x = \frac{1}{c_0 v_0^*} p_x \tag{4}$$

It is possible to use a simple constant closure for the mean flow gradient, i.e. $U_y = \frac{U}{\delta}$ and $U_y = 0$ for y>>1. For x<<1 we need to use the outer solution with $U_y = 0$ and then increase the presence of the non-zero inner gradient for "x" increasing. Thus we propose the model: $U_y = \left(\frac{U}{\delta}\right)\frac{x}{L_t}$ where L_t is the total transition zone length and can write the term $U_y v_x$ as $U_y v_x \approx \left[\left(\frac{U}{\delta}\right)\left(\frac{\delta}{L_t}\right)\frac{x}{\delta}\right]\left[\frac{1}{c_0 v_0^*} p_x\right] \equiv \frac{\alpha_0}{\delta}\left(\frac{x}{\delta}\right)p_x$. This closure is strictly valid for x<<1 since for $\frac{x}{\delta} >> 1$ this would be a secular (unbounded) term. We will perform our analysis for x<<1 (recall that we are modeling the initial condition) and then extend the model to be valid t>1 and x>>1.

A similar modeling proposal might seem appropriate for the $W_z w_x$ term. Rather than relying on isotropic pressure fluctuation model, we alternatively use a quasi-steady approximation from the "z" Euler equation $w_t + U w_x = -p_z$ whereby: $w_x \approx -\frac{1}{U} p_z$. A model for W_z is less apparent in the absence of an obvious "z" convective velocity. We believe that the scaling associated with the $W_z = \frac{\partial W}{\partial z}$ term follows from

the internal structure (wave oscillation) internal to the wave packet as described by the wave number "k". Thus a plausible model for $W_z = \frac{\partial W}{\partial z}$ would be: $W_z \propto Uk$ whereby $W_z w_x \approx k p_z$. Utilizing a similar argument to $U_y v_x$ we introduce the extension such that: $W_z w_x \approx k\left(\frac{z}{\delta}\right)\left(\frac{\delta}{L_t}\right)p_z$. It is convenient to define: $W_z w_x \equiv \frac{\beta_0}{\delta}\left(\frac{z}{\delta}\right)p_z$ where $\beta_0 = k\delta\left(\frac{\delta}{L_t}\right)$. With these approximations/definitions we can formulate the equation:

$$p_{xx} + p_{yy} + p_{zz} + U_y v_x + W_z w_x = 0$$

$$p_{xx} + \frac{\alpha_0}{\delta}\left(\frac{x}{\delta}\right)p_x + p_{zz} + \frac{\beta_0}{\delta}\left(\frac{z}{\delta}\right)p_z + p_{yy} = 0 \tag{5}$$

Equation (5) is linear and separable whereby the expression: $p(x,y,z) = f(x,z)g(y)$ is of use. Applying this expression to equation (5) we then obtain:

$$f_{xx} + \frac{\alpha_0}{\delta}\left(\frac{x}{\delta}\right)f_x + f_{zz} + \frac{\beta_0}{\delta}\left(\frac{z}{\delta}\right)f_z + \mu^2 f = 0$$

$$g'' - \mu^2 g = 0 \tag{6}$$

where μ^2 is the separation constant. The f(x,y) (modified Helmholtz equation) is separable as $f(x,z) = A(x)B(z)$ which yields:

$$A'' + \frac{\alpha_0}{\delta}\left(\frac{x}{\delta}\right)A' + \lambda^2 A = 0$$

$$B'' + \frac{\beta_0}{\delta}\left(\frac{z}{\delta}\right)B' + (\mu^2 - \lambda^2)B = 0 \tag{7}$$

The two ODE's associated with equation (7) can be readily solved if we can assess a value for the separation constants. Indeed if we let $\lambda^2 \equiv \frac{\alpha_0}{\delta^2}$ then $A'' + \frac{\alpha_0}{\delta}\left(\frac{x}{\delta}\right)A' + \lambda^2 A = 0$ solves as:

$$A \propto \exp\left(-\frac{1}{2}\alpha_0\left(\frac{x}{\delta}\right)^2\right) \tag{8}$$

In a similar manner if we let $(\mu^2 - \lambda^2) \equiv \frac{\beta_0}{\delta^2}$ then yields:

$$B \propto \exp(-\frac{1}{2}\beta_0\left(\frac{z}{\delta}\right)^2) \tag{9}$$

This finally gives: $\mu^2 \equiv \frac{\alpha_0 + \beta_0}{\delta^2}$ and $g'' - \mu^2 g = 0$ provides the expected exponential decay as:

$$g \propto \exp(-\sqrt{\alpha_0 + \beta_0}\left(\frac{y}{\delta}\right)) \tag{10}$$

We are then in a position to formulate the initial condition for pressure term as:

$$p_0(x,y,z) \propto \exp(-\frac{1}{2}\alpha_0\left(\frac{x}{\delta}\right)^2 - \frac{1}{2}\beta_0\left(\frac{z}{\delta}\right)^2 - \sqrt{\alpha_0 + \beta_0}\left(\frac{y}{\delta}\right)) \tag{11}$$

The variable α_0 is fully specified as $\alpha_0 = \frac{1}{c_0}\left(\frac{U}{v^*}\right)\left(\frac{\delta}{L_t}\right)$ while $\beta_0 = k\delta\left(\frac{\delta}{L_t}\right)$. Simple order of magnitude analysis[13] suggests that $\frac{U}{v^*} = \frac{\sqrt{2}}{c_f^{1/2}}$ which is O(25-35).

The dimensionless wave number $k\delta$ is perhaps best understood via the dimensionless wave number as $\frac{Uk}{\omega}$. The dominant portion of the spectrum centers on $\frac{Uk}{\omega} = O(1)$ (Taylor hypothesis) the "so-called convective ridge"[14]. The dimensionless wavenumber can be written in terms of the traditional dimensionless frequency, $k\delta = \frac{\omega\delta}{U}$ suggesting that a wide range of frequencies may play a role in the wavenumber spectrum. The frequency spectrum is dominant for $\frac{\omega\delta}{U} = O(1)$ but is characterized by higher frequencies for smaller (inner law) scales by frequencies on the order of O(100-1000). Certainly, $k\delta$ within the boundary layer can be as large as O(100).

Finally, let's estimate the size of the transition zone length L_t. We can readily relate the transition zone length to the (laminar) boundary layer thickness Reynolds number via the Blasius solution[13]: $\mathrm{Re}_\delta = 5\,\mathrm{Re}_x^{1/2}$, the empirical[10,11] expressions $\mathrm{Re}_\lambda = 9\,\mathrm{Re}_x^{3/4}$ and the definition $\mathrm{Re}_{L_t} = 3.3\,\mathrm{Re}_\lambda$.

Combining these expressions gives: $\mathrm{Re}_{L_t} = 3.3(\frac{9}{25^{3/4}})\,\mathrm{Re}_\delta^{3/2} = 2.7\,\mathrm{Re}_\delta^{3/2}$. The ratio $\frac{\mathrm{Re}_{L_t}}{\mathrm{Re}_\delta} = \frac{L_t}{\delta}$ is shown to be $\frac{\mathrm{Re}_{L_t}}{\mathrm{Re}_\delta} = \frac{L_t}{\delta} \approx 6\,\mathrm{Re}_x^{1/4}$ that for a transitional flat plate, Re_x=O(10^5), give $\frac{\mathrm{Re}_{L_t}}{\mathrm{Re}_\delta} = \frac{L_t}{\delta} = O(100)$ which implies that the spatial domain is given by $0 < \frac{x}{\delta} < 100$ with a similar temporal domain. This suggests, that $\alpha_0 = \frac{1}{c_0}\left(\frac{U}{v^*}\right)\left(\frac{\delta}{L_t}\right) \approx O(1/2) - O(1)$ while $\beta_0 = k\delta\left(\frac{\delta}{L_t}\right) \approx O(1) - O(10)$. Clearly, these are rather gross estimates but they are useful to help delineate

There is value in considering equation (11) for a set of relevant parameter values say: α_0=3/4, $\alpha_0 \approx \frac{1}{2}(1/2+1) = \frac{3}{4}$ and β_0=5.5, $\beta_0 \approx \frac{1}{2}(1+10) = \frac{11}{2}$

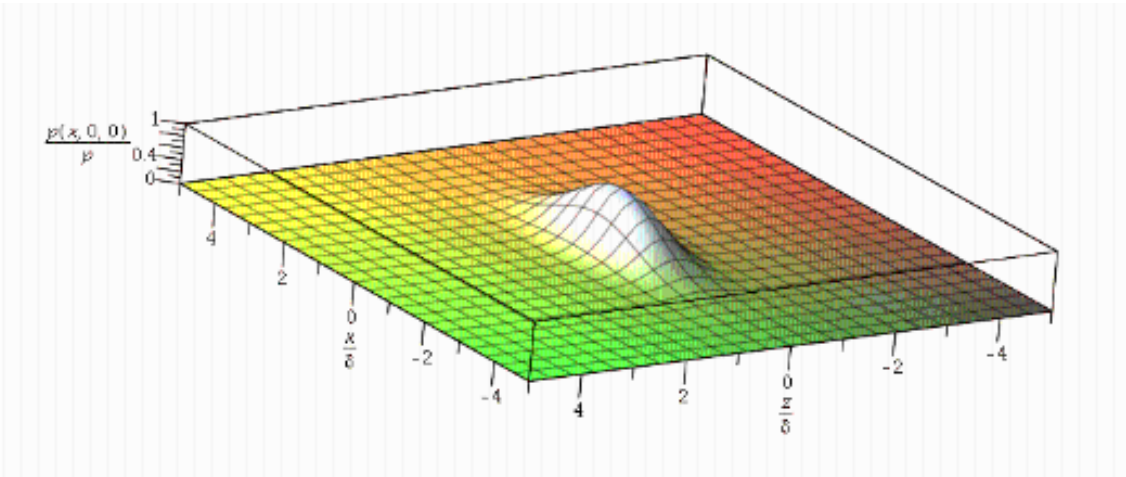

Figure 1. Initial condition p0(x,y,z) for y=0, α0=3/4 and β0=11/2.

These order of magnitude estimates provide useful information regarding the shape of the wave packet magnitude a surrogate for a physical turbulent spot. The spreading rate associated with the spot follows from the ratio of the "x" and "z" expressions in equation (11). Indeed the ratio of the packet footprint width to length is found to be:

$$\tan\phi = \left(\frac{1/\beta_0}{1/\alpha_0}\right)^{1/2} = \left(\frac{\alpha_0}{\beta_0}\right) = O\sqrt{\frac{3}{22}} \rightarrow \phi \approx 21.2° \tag{12}$$

This value compares moderately with the more traditional method of stationary phases spot shape angle result which yields[2,3]: $\phi \approx 19.47°$

Equation (11) can be expected to satisfy the modified Poisson equation: $p_{xx} + p_{yy} + p_{zz} = -U_y v_x - U_z w_x$ modeled as: $p_{xx} + \frac{\alpha_0}{\delta}\left(\frac{x}{\delta}\right)p_x + p_{zz} + \frac{\beta_0}{\delta}\left(\frac{z}{\delta}\right)p_z + p_{yy}$. Equation (11) provides a rational estimate (though a crude one since the shape of the associated spot is upstream/downstream symmetric, clearly not the observed behavior)[3] for the initial condition, let's call it $p_0(x,y,z)$ associated with a single turbulent spot-like wave packet. Certainly turbulent spots are a dynamic phenomenon in a convective flow field as demonstrated by the linearized Euler equations, via equation (1). Using the simple isotropic closure model, i.e. equations (3) and (4) we can readily rewrite the "y" momentum equation as:

$$v_t + Uv_x + c_0 v_0^* v_y = 0 \tag{12}$$

We could as well (using the approximate closure $p = c_0 v^* v$:

$$p_t + Up_x + c_0 v_0^* p_y = 0 \tag{13}$$

Using equation (11) to provide the initial condition: $p_0(x,y,z)$ the solution to equation (13) is (almost) trivial as:

$$\begin{aligned} p(x,y,z,t) &= p_0(\xi,\eta,z) \\ \xi &= x - Ut \\ \eta &= y - v_0^* t \end{aligned} \tag{14}$$

Note that since $\frac{v_0^*}{U} << 1$ that to good approximation: $p_t + Up_x = 0$ whereby: $p(x,y,z,t) = p_0(x-Ut,y,z)$, which simply a streamwise translating impulse with minimal variation. Obviously, this is an idealization since the spot grows in size as it translates.

The preceding analysis discusses the amplitude behavior of the wave packet, but there is no attempt to determine the internal structure of the packet. The internal structure of turbulent spot is characterized by

a complex, stochastic, multiple scale (time and space) unsteady flow behavior. There is virtually no possibility that our simple models will adequately describe this behavior. Nonetheless, the internal structure of the packet is important to us and a meaningful approximation would be of value. Let's consider the linearized Euler equation focusing on:

$$\begin{aligned} u_t + Uu_x + vU_y + wU_z &= -p_x \\ v_t + Uv_x &= -p_y \end{aligned} \tag{15}$$

Let's further introduce $p = c_0 v_0^* v \approx c_0 v_0^* u$ and the scaling approximation $-p_y \approx \frac{p}{\delta}$ which can be combined to give:

$$v_t + Uv_x = \frac{p}{\delta} \rightarrow u = \frac{\delta}{c_0 v^*}\left(v_t + Uv_x\right) \tag{16}$$

Then, assuming that x<<1 we can write: $u_t + (U + c_0 v^*)u_x = 0$ which is approximately: $u_t + Uu_x = 0$. Using equation (16) we can write:

$$u_{tt} + 2Uu_{tx} + U^2 u_{xx} = 0 \tag{17}$$

Though highly simplified equation (17) is intended to an estimate for the internal behavior of the wave packet. Equation (17) admits the solution: $u(x,t) \propto \exp(ik(x-ct))$. We can substitute into equation (17) to estimate a value for c as:

$$k^2(c^2 - 2Uc + U) = 0 \rightarrow c = U \tag{18}$$

Such that $u(x,t) \propto \exp(ik(x-Ut))$ which taking the real part is simply: $u(x,t) \propto \cos(k(x-Ut))$. Thus, a (normalized) wave packet can be modeled as:

$$p \propto \cos(k\delta(\frac{x-Ut}{\delta}))\exp(-\frac{1}{2c_0}\left(\frac{U}{v^*}\right)\left(\frac{x-Ut}{\delta}\right)^2 - \frac{1}{2}k\delta\left(\frac{z}{\delta}\right)^2 - \sqrt{\left(\frac{U}{c_0 v^*}\right) + k\delta\left(\frac{y}{\delta}\right)}) \tag{19}$$

While highly simplified, equation (19) nonetheless may provide a suitable tool to model wave packet behavior. Notice the constraint between packet periodicity $\cos(k\delta(\frac{x}{\delta}))$ e.g. $k\delta$ and the lateral spreading parameter $\beta = k\delta$ implied by equation (19) which suggests a relationship between spot shape and internal periodic structure. This is a relationship that we readily test by comparison to experimental measurement.

Casper et. al.[14] provides a series of compelling measurements for wave packet and turbulent spot structure for supersonic flow over a sharp cone. Figure 6 provides an excellent measurement representation for the

initial behavior of a wave packet and an opportunity to ascertain the overall validity of equation (19) for t<<1. The periodicity of the wave packet in the measurements is approximately $k\delta \approx 10$. Using $\frac{1}{c_0}\left(\frac{U}{v^*}\right)\left(\frac{\delta}{L_t}\right) = O(1)$ equation (19) can be written as $p(x,0,z,0) \propto \cos(10(\frac{x}{\delta}))\exp(-\frac{1}{2}\left(\frac{1}{2}\right)\left(\frac{x}{\delta}\right)^2 - \frac{1}{2}(10)\left(\frac{z}{\delta}\right)^2)$ which

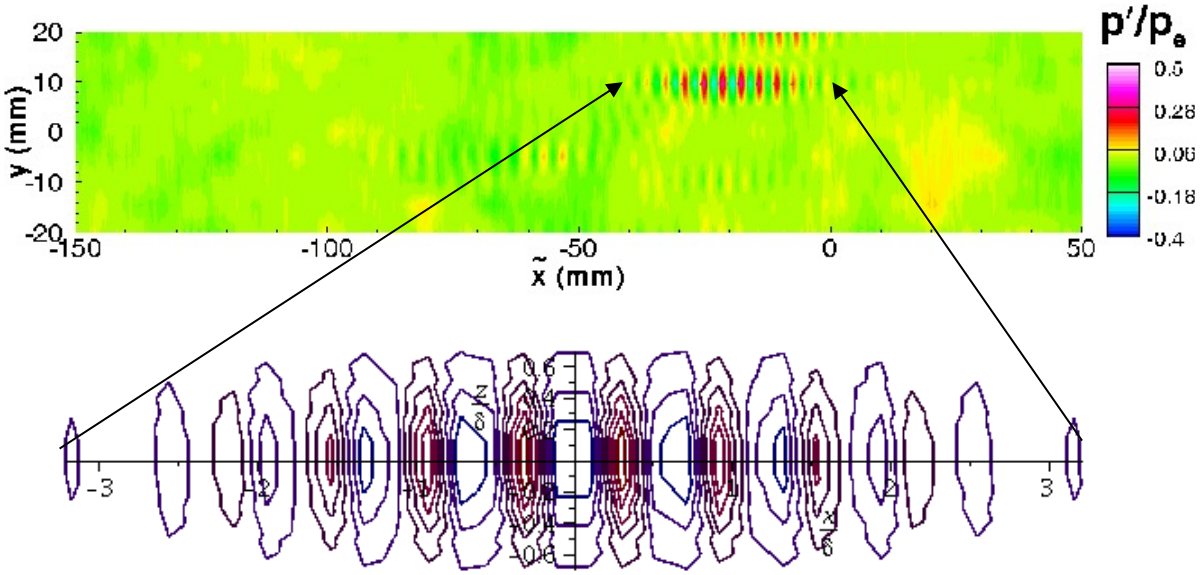

Figure 2. qualitative comparison between measured wave packet and wave packet model

In figure 2 we present a qualitative comparison between measured wave packet[14] and wave packet model: $p(x,0,z,0) \propto \cos(10(\frac{x}{\delta}))\exp(-\frac{1}{2}\left(\frac{1}{2}\right)\left(\frac{x}{\delta}\right)^2 - \frac{1}{2}(10)\left(\frac{z}{\delta}\right)^2)$ for $k\delta \approx 10$ and $\frac{1}{c_0}\left(\frac{U}{v^*}\right)\left(\frac{\delta}{L_t}\right) \approx O(1/2)$.

Measured packet width to length is estimated as: $\frac{10}{50} = \frac{1}{5}$ while analytical value is: $\left(\frac{1}{2}/10\right)^{1/2} \approx 0.224$.

The reduction in friction velocity follows from the traditional[13] mapping from conical to flat plate flows.

B. Wave Packet Pulse Growth

A particular issue with the preceding solution is that the spot translates but retains its shape throughout the flow. For a spot to increase its length in the streamwise direction[3], we need to decrease the size of the

term $-\frac{1}{2c_0}\left(\frac{U}{v^*}\right)\left(\frac{x-Ut}{\delta}\right)^2$ in equation (19). An effective decrease for this term might follow from the method-of-characteristics that was used to estimate the $x-Ut$. This term was derived by solving a simple expression of the form:

$$p_t + Up_x = 0 \quad p(x, t=0) = p_0(x) \tag{20}$$

Which has the solution $p(x,t) = p_0(\xi) = p_0(x-Ut)$ for any function $p_0(x,t)$. Equation (20) follows from "u" momentum equation $u_t + Uu_x + vU_y + wU_z = -p_x$ with $vU_y + wU_z \approx 0$ where we have assumed that U>>1 and that the convective term will dominate.

Let's examine equation (15) $u_t + Uu_x + vU_y + wU_z = -p_x$. We can model $p = c_0 v^* u \rightarrow u = \frac{p}{c_0 v^*}$ and choose a model for vU_y. Certainly a reasonable model for U_y is $U_y \approx \left(\frac{U}{\delta}\right)$. Recall, however, that we noted that x<<1 we need to use the outer solution with $U_y = 0$ and then increase the presence of the non-zero inner gradient for "x" increasing. This lead to the model: $U_y \approx \left(\frac{U}{\delta}\right)\left(\frac{x}{\delta}\right)$ valid for x<< δ To retain simplicity, let's assume that the $\left(\frac{x}{\delta}\right)$ term can be modeled by a dimensionless constant κ where $\kappa = \left(\frac{\delta}{L_t}\right)$ with L_t the total transition zone length.

The closure for "v" is rather less clear. A possibility is: $v = \frac{p}{c_0 v^*}$ so that the governing equation would then become:

$$\begin{aligned} &u_t + Uu_x = -vU_y - p_x \\ &p_t + [c_0 v^* + U]p_x + \kappa\frac{U}{\delta}p \approx p_t + Up_x + \kappa\frac{U}{\delta}p = 0 \end{aligned} \tag{21}$$

Equation (21) can be solved:

$$\begin{aligned} &p(x,t) = p_0(\xi)\exp(-\kappa\frac{U}{\delta}t) \\ &\xi = x - [c_0 v^* + U]t \approx x - Ut \end{aligned} \tag{22}$$

Examination of equation (22) indicates a temporally damped system with disturbance magnitude. This behavior is not consistent with our experience for wave packets whereby structures tend to increase in size[3].

Let's then re-examine the assumptions utilized to achieve equation (21). Consider modifying the "v" expression to be: $v = \frac{x}{c_0 v^*} p_x$. The choice to model in terms of the pressure gradient rather than the pressure itself will have a significant impact on the behavior of the model. It is critical to note that the approximation: $p \approx x p_x$ is (strictly) valid for a local linear approximation only. Certainly this approximation will not be valid over the full domain.

For a convectively dominated flow it is relatively simple for us to modify the expression $p \approx x p_x$ to be a local model by writing: $p \approx \kappa(\frac{x-Ut}{\delta}) p_x$. The governing equation would then take the form:

$$p_t + [U(1+\kappa\frac{x-Ut}{\delta}) + c_0 v^*]p_x = 0$$

$$p_t + U(1+\kappa\frac{x-Ut}{\delta})p_x = 0 \qquad (23)$$

Given an appropriate initial condition $p_0(x)$ we can solve equation (23). The method-of-characteristics approach requires that: $p(x,t) = p_0(\xi)$ and:

$$\frac{dx}{dt} = U(1+\kappa\frac{x-Ut}{\delta}) \quad x(0) = \xi \qquad (24)$$

Equation (23) can be solved for ξ to give: $\xi = (x-Ut)\exp(-\kappa\frac{U}{\delta}t)$ so that $p(x,t) = p_0(\frac{x-Ut}{\delta})\exp(-\kappa\frac{U}{\delta}t))$ for an arbitrary initial condition. Notice, that this approximation has damped the effective length scale associated with solution. Using $\kappa = const\left(\frac{\delta}{L_t}\right)$ we can write: $p(x,t) = p_0(\frac{x-Ut}{\delta})\exp(-const\frac{U}{L_t}t))$. If we apply this kind of approximation to equation (19) and focus only on the streamwise "x" variation we can write:

$$p(x,0,0,0) \propto \exp(-\frac{1}{2c_0}\left(\frac{U}{v^*}\right)\left(\frac{\delta}{L_t}\right)\exp(-const\,\frac{2Ut}{L_t})\left(\frac{x-Ut}{\delta}\right)^2) \qquad (25)$$

This modification will cause the spot to increase in size as it moves in the streamwise "x" direction. The constant $-const\,\frac{2Ut}{L_t}$ is estimated to be O(1). We utilize $const \approx 3$. With this information we can provide a snapshot of the transition zone process where each individual spot/packet is described by:

$$p(x,0,0,0) \propto \exp(-\exp(-6\frac{x_i}{L_t})\left(100\,\frac{x-x_i}{L_t}\right)^2) \qquad (26)$$

where x_i is the location of the spots within the transition domain. Equation (26) is particularly useful since it permits one to make simple time averaged estimates of the pressure behavior within the transition zone. For a computation of this type, details of the wave packet internal structure are of less value as compared to the wave packet magnitude. Further 3-d details in the "y" and "z" directions may also be neglected whereby equation (26) provides a simple spatial model for pressure pulses. By distributing pressure pulses in a manner physically consistent overall with the behavior in a transition zone, e.g. a maximum burst rate near the middle zone, we can approximately emulate both mean square pressure fluctuation and intermittency behaviors which are discussed subsequently.

Finally, while a single pressure pulse (packet) for a given wave number with the sinusoidal internal structure suggested by equation (19), e.g. $p(x,y,z,t) \propto \cos(k\delta(\frac{x-Ut}{\delta}))\exp(-\exp(-6\frac{x_i}{L_t})\left(\frac{x-Ut}{\delta}\right)^2))$ at a particular location does not provide a meaningful pressure distribution for the transition zone, it nonetheless, can support a correlation function and a frequency spectrum. We examine the correlation model and frequency spectrum in the next section.

III. RESULTS AND DISCUSSION

As suggested, a simple model for wavepacket/spot interaction is possible by ignoring temporal and "y" and "z" spot variation. Let's consider a domain where $L_t \approx 100\delta$. Within this domain let's place a series N of turbulent spots. The number of spots, of course, varies but 6-12 spots within the zone seems to be a plausible number[15]. The strength and functional behavior are provided by equation (26). The location and clustering of the spots is suggested by the burst rate formulation which suggests limited laminar

turbulent switching (bursting) for x/δ≈0 and x/δ≈1 with a maximum in between. Depending on the intermittency distribution the maximum can be near x/δ=0.33 or x/δ=0.53[12]. If we choose a maximum symmetrically located, i.e. x/δ=1/2 and N=10 we will place spots at: $\frac{x_i}{L_t} = (0.25,0.375,0.417,0.458,0.5,0.542,0.583,0.625,0.75,1.0)$ and then sum the resulting expression to provide a net pressure expression. Note that the packets in increase in length for increasing x/δ according to $\exp(-\exp(-6\frac{x_i}{L_t}))$ which causes the additive interference for 50<x/δ<100.

The figure provides a rather gross explanation for the observed local increase in RMS pressure fluctuation as compared to the fully developed RMS pressure in the transition zone. Indeed, if we utilize a model developed in DeChant[9] which estimates that the ratio of the transition pressure magnitude as:

$$\frac{p_{trans}}{p_{FD}} = 14\left(\frac{x}{L_t}\right)^3 (1-\gamma(\frac{x}{L_t})) + \gamma(\frac{x}{L_t}) \tag{27}$$

with the intermittency model $\gamma(\frac{x}{L_t}) = 1-\exp(-4.6052\left(\frac{x}{L_t}\right)^3)$ to the fully turbulent value we can plot the expression in figure 3.

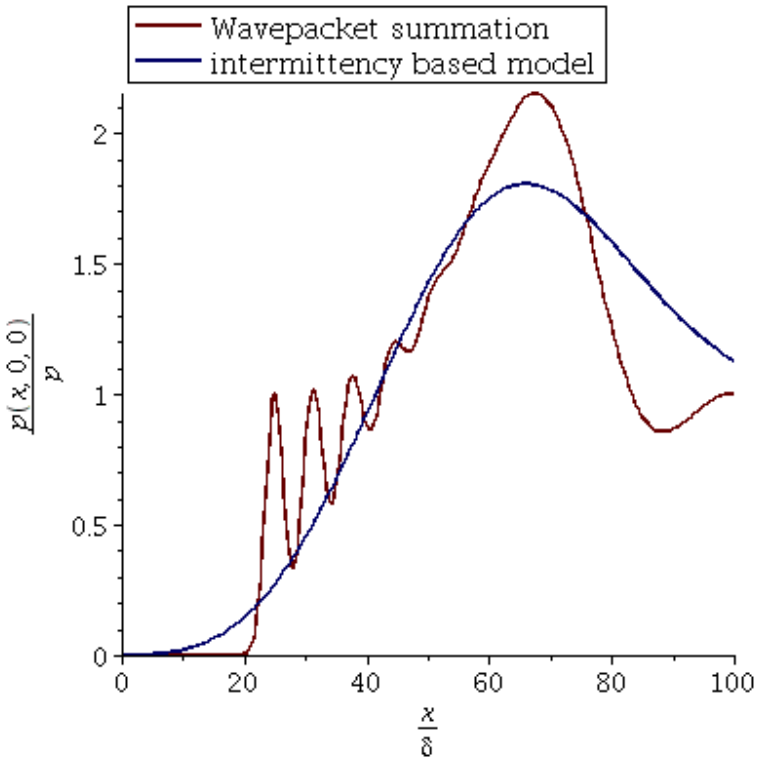

Figure 3. Comparison between RMS pressure wave packet summation model and intermittency based model.

Here we provide a comparison between RMS pressure wave packet summation model and intermittency based expression: $\frac{p_{trans}}{p_{FD}} = 14\left(\frac{x}{L_t}\right)^3 (1-\gamma(\frac{x}{L_t})) + \gamma(\frac{x}{L_t})$. Though the model only roughly estimates pressure loading for x/δ>60 it grossly suggests a plausible agreement between the two approaches.

With estimates of the pressure field available and the fact that a non-zero pressure response corresponds to a turbulent zone we are in a position to coarsely estimate the intermittency, i.e. the fraction of the flow that is turbulent relative to total flow[10,11]. This estimate flows by integral averaging the net pressure function as:

$$\gamma \approx \frac{1}{x/L_t} \int_0^{x/L_t} \frac{p(s,0,0)}{p_{FD}} ds \qquad (28)$$

This integration if performed over the domain associated with the transition behavior. Using the pressure expression defined earlier and the distribution:

$\frac{x_i}{L_t} = (0.25,0.375,0.417,0.458,0.5,0.542,0.583,0.625,0.75,1.0)$ we can estimate the intermittency and plot the result as compared to the analytical model $\gamma(\frac{x}{L_t}) = 1 - \exp(-4.6052\left(\frac{x}{L_t}\right)^3)$ as:

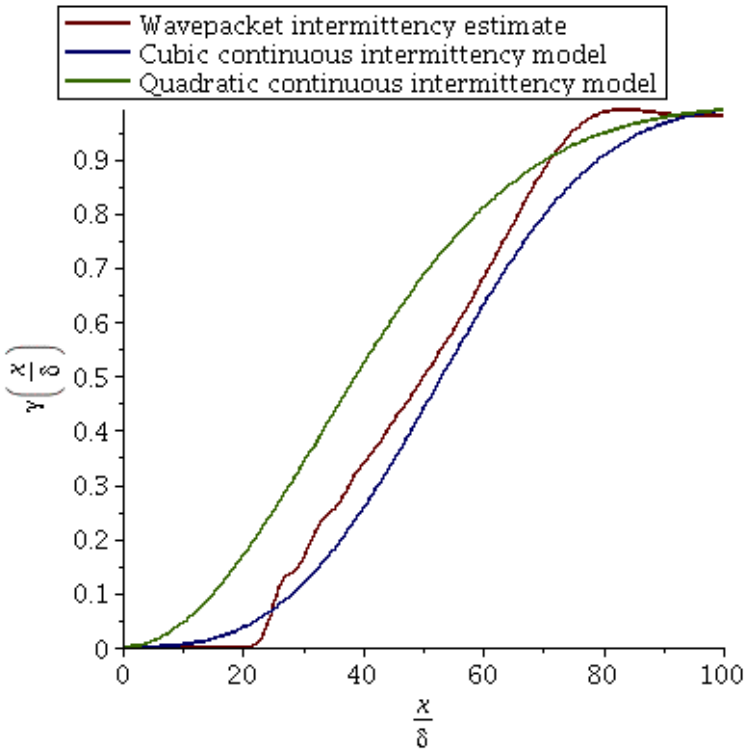

Figure 4. Intermittency estimate using integral definition compared to cubic and quadratic estimates.

In figure 4 we specifically compare intermittency estimate using integral definition: $\gamma \approx \frac{1}{x/L}\int_0^{x/L} \frac{p(s,0,0)}{p_{FD}} ds$ compared to cubic $\gamma(\frac{x}{L_t}) = 1 - \exp(-4.6052\left(\frac{x}{L_t}\right)^3)$ and quadratic $\gamma(\frac{x}{L_t}) = 1 - \exp(-4.6052\left(\frac{x}{L_t}\right)^2)$ intermittency models[10,11]. Figures 3. and 4. suggest that global quantities such as the root-mean-square pressure fluctuation distribution and the intermittency can be adequately approximated in 2-d by a steady distribution of pressure pulse packets.

As suggested previously it is possible, as well, to examine the auto-correlation (longitudinal spatial correlation function assuming Taylor's hypothesis is valid) and the attendant frequency spectrum (power-spectral-density) for a single wave packet. Consider the packet described by:

$$p(x,y,z,t) = \cos(k\delta(\frac{x-Ut}{\delta}))\exp(-\exp(-6\frac{x_i}{L_t})\left(\frac{x-Ut}{\delta}\right)^2)) \tag{29}$$

For x=0 we can readily compute the autocorrelation as:

$$\begin{aligned} R(k\delta,\frac{U\tau}{\delta}) &\propto \int_{-\infty}^{\infty}[\cos(kUt))\exp(-\left(\frac{Ut}{\delta}\right)^2)][\cos(kU(t+\tau))\exp(-\left(\frac{U(t+\tau)}{\delta}\right)^2)]dt \\ &\propto \exp(-\frac{1}{2}((\frac{U\tau}{\delta})^2-(k\delta)^2)[\cos(k\delta\frac{U\tau}{\delta})\exp(\frac{1}{2}(k\delta)^2)+1] \end{aligned} \tag{30}$$

Notice, that the auto-correlation is a function of the packet wave number "k" or the dimensionless form "kδ". The resulting expression is in the form of a damped sinusoidal function which yields: $R(k\delta,\frac{U\tau}{\delta}) \propto \exp(-\frac{1}{2}(\frac{U\tau}{\delta})^2)$ for kδ<<1 and tends towards $R(k\delta,\frac{U\tau}{\delta}) \propto \frac{\sqrt{2\pi}}{4}\exp(-\frac{1}{2}((\frac{U\tau}{\delta})^2)\cos(k\delta\frac{U\tau}{\delta})$ for kδ>>1.

Using the Fourier-transform pair that connects the auto-correlation to the power spectral density[15] (also called the frequency spectrum or auto-spectral density) we can compute power spectral density as:

$$\begin{aligned} \Phi(\frac{\omega\delta}{U},k\delta) &\propto \int_{-\infty}^{\infty}R(k\delta,\frac{U\tau}{\delta})\cos(\omega\tau)d\tau \\ &\propto [\exp((k\delta\frac{\omega\delta}{U})+1]^2\exp[-\frac{1}{2}(k\delta+\frac{\omega\delta}{U})^2] \end{aligned} \tag{31}$$

For small wave number kδ the result is simply $\Phi \propto \exp[-\frac{1}{2}(\frac{\omega\delta}{U})^2]$ which is largely consistent with the Lowson[7] classical result $\Phi \propto \frac{1}{1+(\frac{\omega\delta}{U})^2}$.

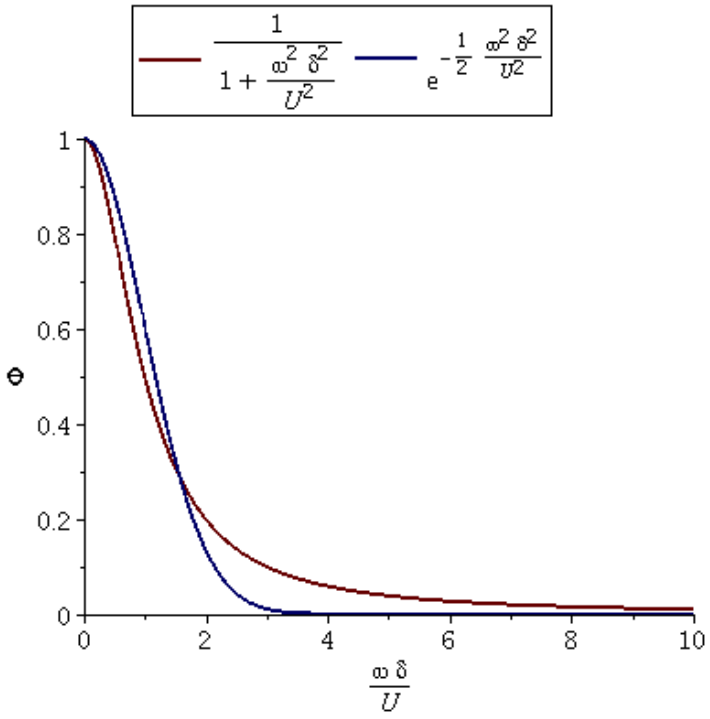

Figure 5. Comparison between scaled low frequency power spectral density models.

In figure 5 we provide a comparison between scaled low frequency power spectral density models, i.e. Lowson[8] $\Phi \propto \frac{1}{1+(\frac{\omega\delta}{U})^2}$ and packet model $\Phi \propto \exp[-\frac{1}{2}(\frac{\omega\delta}{U})^2]$. For kδ>>1we have $\Phi \propto \exp[(k\delta)(\frac{\omega\delta}{U}) - \frac{1}{2}((k\delta)^2 + (\frac{\omega\delta}{U})^2)+]$ The form of the large wave number expression implies that $\Phi = O(1)$ for $\frac{\omega\delta}{U} \approx k\delta$ and is zero elsewhere. This frequency behavior is consistent with a correlation function of the form: $R(k\delta, \frac{U\tau}{\delta}) \approx \cos(k\delta \frac{U\tau}{\delta})$ where one formally recovers the well-known result that the frequency spectrum is simply a Dirac delta solution with $\frac{\omega\delta}{U} \approx k\delta$. From this analysis we can conclude that the wave packet model provides useful correlation/spectral results in the low frequency range, but is rather less useful as a tool to provide information in the high frequency range.

IV. CONCLUSION

We have derived an approximate but explicit model for transitional pressure fluctuation behavior by approximately solving the linearized Euler equations and using a kinematic wave initial value problem formulation. The initial value for this computation followed from a modified pressure Poisson equation formulation supplemented by a simple semi-empirical linearized expression to map between pressure fluctuation and velocity fluctuation. Streamwise variation of the mean flow component was explicitly included. Solving the resulting linear variable coefficient partial differential equation yielded a plausible wave packet initial amplitude expression that combined with the convective dominated kinematic wave solution resulted in a complete unsteady packet amplitude model. For a given wave number, the internal structure of the packet was shown to be sinusoidal in structure. The overall packet model needed to be extended to honor the streamwise growth of the disturbance. The wave packet pressure fluctuation model provided approximate, but physics-based modeling for the transition layer pressure field including the root-mean-square pressure fluctuation behavior models, an estimate for the intermittency, pressure fluctuation auto-correlation and frequency spectrum. Application of the model to these problems suggests that, even though the wave packet model derived here is certainly approximate in nature, it provides a simple explicit formulation for pressure behavior.

V. REFERENCES

[1]Courant, R., Hilbert, D. *Methods of Mathematical Physics*, 2nd ed. New York, Wiley Interscience 1953.

[2]Bowles, R. G. A, Smith, F. T. "Short-Scale Effects on Model Boundary-Layer Spots," Journal of Fluid Mechanics, Vol. 295, pp 395-407, 1995.

[3]Schmid, P. J., Henningson, D. S., *Stability and Transition in Shear Flows*, Springer, New York, 2001.

[4]Cohen, J., Breuer, K. S., Haritonidis, J. H., "On the Evolution of a Wave Packet in a Laminar Boundary Layer," *Journal of Fluid Mechanics*, Vol. 225, pp. 575-606, 1991.

[5]Kachanov, Y. S., Lechenko, V. Y., "The Resonant Interaction of Disturbances at Laminar-Turbulent Transition in a Boundary Layer," *Journal of Fluid Mechanics*, Vol. 138 pp. 209-247, 1984.

[6]Breuer, K. S., Cohen, J., Haritonidis, J. H., The Late Stages of Transition Induced by a Law-Amplitude Wave Packet in a Laminar Boundary Layer, *Journal of Fluid Mechanics*, to appear, 2015.

[7]Lowson, M. V. "Pressure Fluctuation in Turbulent Boundary Layers," NASA TN D-3156 1965.

[8]Lowson, M. V., "Prediction of Boundary Layer Pressure Fluctuations," AFFDL-TR-67, April, 1968.

[9]DeChant, L. J., "An Incompressible RMS Pressure Fluctuation Model Using Inner Law Concepts with Extensions to Laminar-Turbulent Transitional Flow," submitted 6/2014 to AIAA

[10]Dhawan, S. and Narasimha, R., "Some Properties of Boundary Layer Flow During the Transition from Laminar to Turbulent Motion," Journal of Fluid Mechanics, Vol. 3, No. 4, 1958, pp. 418–435.

[11]Narasimha, R., "The Laminar-Turbulent Transition Zone in the Boundary Layer," Progress in Aerospace Sciences, Vol. 22, January 1985, pp. 29–80.

[12]Dechant, L. J., "Laminar Turbulent Intermittency Models: Determination of Functional Behavior Using an Asymptotic Differential Equation Argument." submitted 6/2014 to AIAA Scitech2015, 01-05-2015, Kissimmee, FL, 2015.

[13]White, F. M., *Viscous Fluid Flow, 3rd ed*., Mc Graw-Hill, New York, 2006.

[14]Casper, K. M., Beresh, S. J, Henfling, J. F., Spillers, R. W., Pruett, B. O., "High-Speed Schlieren Imaging of Disturbances in a Transitional Hypersonic Boundary Layer," AIAA-2013-0376

[15]Blake, W. K., *Mechanics of Flow Induced Sound*, Vol. I and II, Academic Press, London, 1986.

VI. DISTRIBUTION

1	MS0346	Richard Field	1526 (electronic copy)
1	MS0346	Mikhail Mesh	1523 (electronic copy)
1	MS0825	Steven Beresh	1515 (electronic copy)
1	MS0825	Lawrence DeChant	1515 (electronic copy)
1	MS0825	Jeff Payne	1515 (electronic copy)
1	MS0825	Justin Smith	1515 (electronic copy)
1	MS9018	Central Technical Files	8944 (electronic copy)
1	MS0899	Technical Library	4536 (electronic copy)


Sandia National Laboratories